Macromolecules

ARTICLE

pubs.acs.org/Macromolecules

Phase Diagrams of Blends of Polyisobutylene and Deuterated Polybutadiene as a Function of Chain Length

Alisyn J. Nedoma,[†] Peggy Lai,[†] Andrew Jackson,[‡,§] Megan L. Robertson,[†] Nisita S. Wanakule,[†] and Nitash P. Balsara*[,†,∥,⊥]

[†]Department of Chemical Engineering, University of California, Berkeley, Berkeley, California 94720, United States

[‡]National Institute of Standards and Technology Center for Neutron Research, Gaithersburg, Maryland 20899, United States

[§]Department of Materials Science and Engineering, University of Maryland, College Park, Maryland 20742, United States

[∥]Materials Sciences Division, Lawrence Berkeley National Laboratory, Berkeley, California 94720, United States

[⊥]Environmental Energy Technologies Division, Lawrence Berkeley National Laboratory, Berkeley, California 94720, United States

Supporting Information

ABSTRACT: Phase diagrams of four binary blends of polyisobutylene (component 1) and deuterated polybutadiene (component 2) were determined using small-angle neutron scattering (SANS). Our study covers N_1/N_2 values ranging from 0.23 to 0.92 and N_i ranging from about 800 to 3600 (N_i is the number of monomers per chain of component i based on a reference volume = 0.1 nm^3). The experimentally determined binodal curves were in good agreement with the predictions based on the Flory−Huggins theory using a previously determined composition- and chain-length-dependent Flory−Huggins interaction parameter presented in Nedoma et al. et al. Macromolecules 2008, 41, 5773−5779. The experimentally determined spinodal curves, which were surprisingly close to the experimental binodal curves, deviated significantly from predictions, an observation for which we offer no quantitative explanation.

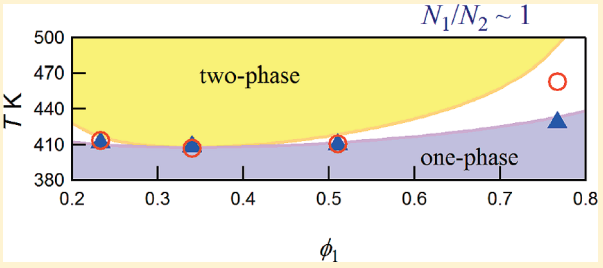

INTRODUCTION

This paper deals with experimental observations of the phase behavior of binary blends of two model polyolefins: polysiobutylene (PIB) and deuterated polybutadiene (dPBD). The fact that the phase behavior of mixtures of two polymers labeled 1 and 2 depends on the chain lengths of the components, N_1 and N_2, respectively, has been known since the development of the Flory−Huggins theory.[1,2] Previous studies in this area,[3−13] however, are restricted to narrow ranges for N_1 and N_2. In fact, most of the studies are restricted to a single pair of homopolymers with nearly equal chain lengths ($N_1/N_2 \approx 1$).

In principle, the Flory−Huggins interaction parameter, χ, accounts for enthalpic interactions between different polymer species. This leads to a χ parameter that only depends on temperature (we ignore pressure effects in this paper). Small-angle neutron scattering (SANS) from homogeneous blends has emerged as a powerful method for determining the χ parameter.[14] In many studies, however, the χ obtained from SANS depends on composition (ϕ_1)[3−13] or chain length (N_1 and N_2)[5,15,16] due to other effects such as specific interactions, local packing, thermal properties, etc.

In a previous paper,[17] we reported χ parameters obtained from a series of homogeneous PIB/dPBD blends. The distinguishing feature of this study was that it covered a wide range of blend compositions and chain lengths. We used the random phase approximation[14] to obtain χ from SANS data measured from homogeneous blends. The average chain length, N_{AVE}, defined as $N_{AVE} \equiv 4[1/N_1^{1/2} + 1/N_2^{1/2}]^{-2}$, is useful for organizing the data obtained from these blends. Blends with $N_{AVE} \leq 580$ (we use a reference volume = 0.1 nm^3) were homogeneous across the entire experimental temperature window (303−473 K). In contrast, blends with $N_{AVE} \geq 950$ exhibited a homogeneous-to-two-phase transition as they were heated. In this paper, we report on the phase behavior of PIB/dPBD blends with $N_{AVE} \geq 950$. We compare the experimentally determined phase diagram with predictions based on the χ parameters reported previously in ref 17 that were consistent with data obtained across the entire N_{AVE} range.

THEORY

The Gibbs free energy of mixing per volume, ΔG, is given by the Flory−Huggins equation:[1,2]

$$\frac{\Delta G v_0}{kT} = \frac{\phi_1 \ln \phi_1}{N_1} + \frac{(1-\phi_1)\ln(1-\phi_1)}{N_2} + \chi\phi_1\phi_2 \qquad (1)$$

Received: February 4, 2011
Revised: March 1, 2011
Published: March 25, 2011

where v_0 is a reference volume which we fix at 0.1 nm^3, ϕ_i is the volume fraction of species i in the blend, N_i is the temperature-dependent number of repeat units of volume v_0 on a single chain of species i, and χ is the Flory–Huggins interaction parameter.

The coexisting compositions at a given temperature are given by the common tangent construction:

$$\left.\frac{d\Delta G}{d\phi_1}\right|_{\phi_1^I} = \left.\frac{d\Delta G}{d\phi_1}\right|_{\phi_1^{II}} = \frac{\Delta G_{\phi_1^I} - \Delta G_{\phi_1^{II}}}{\phi_1^I - \phi_1^{II}} \quad (2)$$

where ϕ_1^I and ϕ_1^{II} are the volume fractions of polymer 1 in the coexisting phases I and II, respectively.

The limit of thermodynamic stability, the spinodal curve, is given by

$$\frac{\partial^2 \Delta G}{\partial {\phi_1}^2} = 0 \quad (3)$$

and the critical point is given by the simultaneous solution of eqs 3 and 4:

$$\frac{\partial^3 \Delta G}{\partial {\phi_1}^3} = 0 \quad (4)$$

Flory–Huggins theory (eqs 1, 3, and 4) gives the volume fraction of species 1 at the critical point:

$$\phi_{1,crit,FHT} = \frac{1}{1 + (N_1/N_2)^{1/2}} \quad (5)$$

The measurement of a thermodynamically robust χ enables computation of the complete phase diagram for a binary polymer blend. SANS is commonly used to measure χ for polymer pairs because the coherent scattering intensity can be related to thermodynamically relevant quantities. Thermal fluctuations in the local composition of the blend are characterized by an effective interaction between homopolymer species, χ_{sc}. The structure factor for the blend, $S(q)$, which arises due to these fluctuations, is usually described by the mean-field random phase approximation (RPA):[14]

$$S(q) = v_0\left[\frac{1}{N_1\phi_1 P_1(q)} + \frac{1}{N_2\phi_2 P_2(q)} - 2\chi_{sc}\right]^{-1} \quad (6)$$

where $\phi_2 = 1 - \phi_1$, q is the magnitude of the scattering vector, and the single chain form factor for each homopolymer is given by the Debye function

$$P_i(q) = \frac{2}{{x_i}^2}(\exp(-x_i) + x_i - 1) \quad (7)$$

with $x_i = q^2 {R_{g,i}}^2$ and ${R_{g,i}}^2 = N_i {l_i}^2/6$. $R_{g,i}$ is the radius of gyration for a chain of species i, and l_i is the statistical segment length.

The static structure factor given by eq 6 can be obtained from the measured coherent scattering intensity and the calculated scattering contrast:

$$I(q) = \Delta\rho^2 S(q) \quad (8)$$

where $\Delta\rho^2 = (b_1/v_1 - b_2/v_2)^2$ is the scattering contrast per volume. The scattering length per monomer of species i, b_i, is computed from the atomic composition of a monomer unit, and v_i is the monomer volume of species i. When these quantities are known, the measured SANS intensity profile can be fitted by the RPA (eqs 6–8) to obtain χ_{sc}.

The structure factor at zero scattering angle, $S(0)$, is related to the second derivative of free energy:

$$S(0)^{-1} = \frac{d^2(\Delta G/kT)}{d{\phi_1}^2} \quad (9)$$

Differentiating the Flory–Huggins free energy from eq 1 yields

$$\frac{1}{S(0)} = \frac{1}{v_0}\left(\frac{1}{N_1\phi_1} + \frac{1}{N_2\phi_2} - 2\chi_{sc}\right) \quad (10)$$

At the spinodal temperature, $S(0)^{-1}$ vanishes, and the value of χ_{sc} at the spinodal temperature is given by

$$\chi_{sc,s} = \frac{1}{2}\left(\frac{1}{N_1\phi_1} + \frac{1}{N_2\phi_2}\right) \quad (11)$$

so that eq 10 may be rewritten as

$$\frac{1}{S(0)} = \frac{2}{v_0}(\chi_{sc,s} - \chi_{sc}) \quad (12)$$

χ_{sc} is usually presumed to be independent of composition and molecular weight with an empirical temperature dependence given by $\chi_{sc} = A + B/T$. For this simple case, the measured value of χ_{sc} is identical to the thermodynamic parameter, χ, in eq 1, and $S(0)^{-1} \sim |{T_s}^{-1} - T^{-1}|$. However, when χ_{sc} is a function of composition, it is no longer identical to χ. Following Sanchez,[18] we obtain χ from χ_{sc} by solving the following differential equation with appropriate boundary conditions

$$\chi_{sc} = -\frac{1}{2}\frac{\partial^2[\phi_1(1-\phi_1)\chi]}{\partial {\phi_1}^2} \quad (13)$$

In our previous studies on PIB/dPBD blends,[17,19] we showed χ_{sc} to be of the form

$$\chi_{sc} = A_{sc}(T) + B_{sc}(T)\frac{2\phi_1 - 1}{N_{AVE}} \quad (14)$$

where $N_{AVE} \equiv 4[1/{N_1}^{1/2} + 1/{N_2}^{1/2}]^{-2}$ is defined at 296 K, and A_{sc} and B_{sc} have the temperature-dependent form $a + b/T + c/T^2$. The empirical expression for χ_{sc} is

$$\chi_{sc}(\phi_1, N_{AVE}, T) = [-0.00622 + 10.6/T - 3040/T^2] \pm 11.3\% + (2\phi_1 - 1)/N_{AVE}[-2.17 + 1910/T - 687000/T^2] \pm 26.2\% \quad (15)$$

The uncertainty in χ_{sc} is estimated as described in ref 10 and attributed to two main factors that are assumed to be independent: (1) the uncertainty in the determination of N_1 and N_2 which we take to be 5% and (2) the uncertainty of the linear regression of χ_{sc} vs $(2\phi_1 - 1)/N_{AVE}$ data presented in ref 17, which we estimate using a Student-T distribution and a 95% confidence interval. A variety of expressions for χ_{sc} were examined in ref 17, and eq 15 was found to be the best empirical fit to χ_{sc} parameters measured from nine different polymer pairs prepared at several different compositions.

The solution of eq 13, obtained by Sanchez,[18] is

$$\chi = \frac{2}{1-\phi_1}\int_0^{1-\phi_1}(1-\phi_1')\chi_{sc}(\phi_1')\, d(1-\phi_1') + \frac{2}{\phi_1}\int_0^{\phi_1}(\phi_1')\chi_{sc}(\phi_1')\, d\phi_1' \quad (16)$$

It is straightforward to show that if χ_{sc} is a linear function of ϕ_1, then χ is also a linear function of ϕ_1. We obtain an expression for

the composition dependence of the measured interaction parameter:

$$\chi = A_{sc}(T) + \frac{1}{3}B_{sc}(T)\frac{2\phi_1 - 1}{N_{AVE}} \quad (17)$$

From comparison of eqs 14 and 17, it is apparent that the sole difference between the measured χ_{sc} and the thermodynamic χ is a factor of 1/3 multiplying the composition-dependent term in eq 17. The corresponding expression for χ is

$$\chi(\phi_1, N_{AVE}, T) = [-0.00622 + 10.6/T - 3040/T^2] \pm 11.3\% + (2\phi_1 - 1)/N_{AVE}[-0.722 + 638/T - 229000/T^2] \pm 26.2\% \quad (18)$$

Equations 1, 2, 3, and 18 are used to predict the binodal and spinodal curves of the blends studied in this paper with no adjustable parameters.

EXPERIMENTAL METHODS

Component 1, polyisobutylene (PIB), was synthesized cationically. Component 2, deuterated polybutadiene (dPBD) with 63% 1,2 addition of the 1,3-butadiene monomers, was synthesized anionically and saturated under high pressure. Details of the synthesis and characterization have been published previously.[20,21] Characteristics of the homopolymers are listed in Table 1. The minor difference in the extent of deuteration of the two dPBD samples is not expected to have a significant effect on blend thermodynamics.[22,23]

Four series of blends were created, representing all possible combinations of the PIB and dPBD homopolymers listed in Table 1. The series were named S[*XX*], where *XX* was the value N_1/N_2. Within each series, four compositions were selected for study including: $\phi_{1,crit,FHT}$ (eq 5), $\phi_{1,crit,pred}$, the critical composition predicted using the empirical χ parameter of the form of eq 18, and two off-critical compositions as noted in Table 2. Additional compositions were studied for the S[0.29] series (see Table 2).

Blends were homogenized by dissolving the two components together into hexane. The samples were precipitated into a 1:1 solution of methanol and acetone, placed atop a quartz window inside an annular aluminum spacer with inner diameter 17 mm, and dried under vacuum at 363 K for 2 days. The sample was enclosed within a second quartz window, and the perimeter was sealed with heat-resistant epoxy except for a small gap on one side to allow thermal expansion of the polymers. Samples were heated under vacuum at 363 K for an additional hour to erase shearing effects caused during preparation. This protocol ensured isotropic scattering.

SANS measurements were carried out on the NG7 and NG3 beamlines at the National Institute of Standards and Technology Neutron Research Center in Gaithersburg, MD. Samples were heated in the beamline from 303 to 463 K in 20 K increments with a 10 min anneal after each temperatures step. Previous work with this system[17,19,20] has shown that this protocol is sufficient to ensure thermal equilibrium. At 463 K all samples were opaque, indicating macrophase separation. The samples were removed from the SANS instrument and slowly cooled to room temperature, becoming clear after several hours. A second heating run was performed in the vicinity of the observed phase transition with 2 K heating increments and a 5 min anneal after each temperature step, also shown to be sufficient to attain thermal equilibrium. SANS data were corrected for background, empty cell, transmission, incoherence due to nonuniform deuteration, and the form factor of the deuterated species, and the data were integrated azimuthally to render I vs q profiles ($q = 4\pi \sin(\theta/2)/\lambda$ in which θ is the scattering angle and λ is the wavelength of incident neutrons).[25]

Table 1. Characterization of Homopolymers

polymer	M_w[a] (kg/mol)	PDI	ρ (g/mL)[b] at 296 K	N at 296 K	n_D
PIB1	44.6	1.04	0.914_0	$0.81_0 \times 10^3$	
PIB2	56.8	1.02	0.914_4	$1.03_1 \times 10^3$	
dPBD1	62.0	1.01	0.918_7	$1.12_0 \times 10^3$	3.65
dPBD2	197.2	1.02	0.912_3	$3.58_9 \times 10^3$	3.04

[a] The weight-averaged molecular weight, M_w, and the polydispersity index, PDI, were both measured using gel permeation chromatography and a Viscotek[24] triple detector array. [b] A methanol−ethylene glycol density gradient column, isothermal at 296 K, was used to measure density and thereby calculate the number of deuterium atoms per C_4 monomer unit, n_D.

RESULTS AND DISCUSSION

SANS profiles were measured for each blend as the sample was heated from the one phase to the macrophase separated region. Profiles within the homogeneous phase window exhibited a plateau at low q values, indicating single-phase behavior. With the onset of macrophase separation there was an upturn in the low q scattering. The temperature at which this upturn occurs, T_b, indicates the critical point in the case of critical blends. For off-critical blends, T_b, may be elevated relative to the "true" binodal temperature due to nucleation barriers. Figure 1 shows the SANS profiles for the blend predicted to be critical ($\phi_1 = \phi_{1,crit,pred} = 0.44$) of the series S[0.29] at temperatures near the macrophase separation transition.

In the limit of $R_g^2q^2 \ll 1$, the low-q scattering is described by the Ornstein−Zernike approximation:

$$S(q) = \frac{S(0)}{1 + \xi^2 q^2} \quad (19)$$

where ξ is the correlation length of composition fluctuations. The Ornstein−Zernike structure factor is related to the SANS intensity by eq 8, where $\Delta\rho^2$ is a temperature-dependent quantity because the monomer volumes change as $v_1 = v_1(296\text{ K})\exp[5.7 \times 10^{-4}(T - 296\text{ K})]$ and $v_2 = v_2(296\text{ K})\exp[7.2 \times 10^{-4}(T - 296\text{ K})]$.[26] The monomer volumes at 296 K are calculated for each polymer from the parameters listed in Table 1. While N_i is a function of temperature, N_{AVE} is constant for each blend defined at 296 K, and ϕ_1 changes negligibly. Ornstein−Zernike fits to the one-phase

Table 2. Blend Characteristics

series	comp 1	comp 2	N_1/N_2[a]	N_{AVE}[a]	ϕ_1 values studied[a]
S[0.92]	PIB2	dPBD1	0.92_1	$1.07_5 \times 10^3$	0.23_3, 0.33_9, 0.51_0, 0.76_7
S[0.72]	PIB1	dPBD1	0.72_3	$0.94_7 \times 10^3$	0.26_7, 0.36_9, 0.54_0, 0.73_3
S[0.29]	PIB2	dPBD2	0.28_8	$1.75_0 \times 10^3$	0.23_8, 0.30_0, 0.43_9, 0.50_0, 0.60_0, 0.65_1, 0.76_2
S[0.23]	PIB1	dPBD2	0.22_6	$1.48_9 \times 10^3$	0.27_2, 0.46_8, 0.67_8, 0.72_8

[a] Values reported at 296 K.

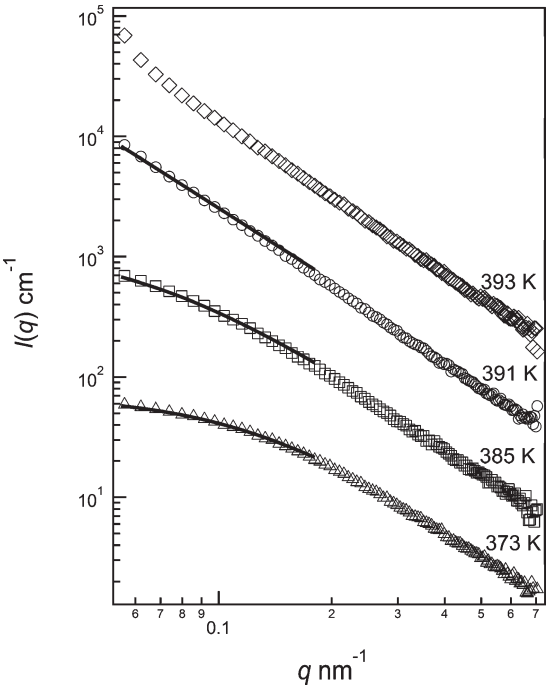

Figure 1. SANS profiles for blend S[0.29] with $\phi_1 = 0.44$ at selected temperatures. Solid lines are Ornstein−Zernike fits to the low q data. Profiles are shifted 0 cm^{-1} (373 K), 14 000 cm^{-1} (385 K), 29 000 cm^{-1} (391 K), and 45 000 cm^{-1} (393 K).

Table 3. Ornstein−Zernike Fitting Parameters for S[0.29] with $\phi_1 = 0.44$[a]

T, K	$S(0)$, nm^3	ξ, nm
373	89	8.32
385	323	15.7
391	28400	146

[a] These parameters correspond to the fits shown in Figure 1.

SANS intensity profiles are shown in Figure 1, and the corresponding fitting parameters are listed in Table 3. A full list of $S(0)$ and ξ values is available for all blends and temperatures studied in the Supporting Information section 1. Equation 15 may be viewed as the simplest expression that we were able to obtain to describe all of the measured values of $S(0)$.

Ornstein−Zernike fits of the SANS data provide an experimentally measured susceptibility that is directly proportional to χ_{sc} (eq 12). In Figure 2 we plot the experimental quantity ${}^1/_2 v_0 S(0)^{-1}$ against the calculated quantity $-\chi_{sc}$ for selected blends. The abscissa is a convenient choice for comparing blends with different values of ϕ_1 and N_{AVE} because it incorporates these dependences into a single parameter, χ_{sc}. The ordinate was chosen to give a linear correlation that intercepts the y-axis at $\chi_{sc,s}$ and has a slope of 1, evident by rearranging eq 12. Parameters for the linear fits shown in Figure 2 are listed in Table 4. The slopes vary between 0.80 and 1.10, in agreement with the expected value of 1, and $\chi_{sc,s}$ varies from 0.000 98 to 0.002 66.

If we consider the susceptibility of a single blend, ϕ_1 and N_{AVE} are constant, requiring us only to consider the temperature dependence of χ_{sc}. The measured χ_{sc} for PIB/dPBD is a quadratic function of $1/T$, leading to $S(0)^{-1} \propto a + b/T + c/T^2$. The susceptibility for a blend is finite within the homogeneous phase window and vanishes at the spinodal temperature, T_s. Figure 3 shows quadratic fits to the susceptibility versus $1/T$ for selected blends. The x-axis intercept of the quadratic fit, $S(0)^{-1} = 0$, gives T_s. The magnitude of the calculated error in T_s, given by the uncertainties in a, b, and c, varies unsystematically from sample to sample and ranges from 1 to 30 K. This mean-field approach to determining T_s is contrasted with an alternate approach, the use of critical scaling law fits, in the Supporting Information section 2. For the critical blends, the T_s values determined using scaling laws are within 1 K of those obtained from the quadratic fits.

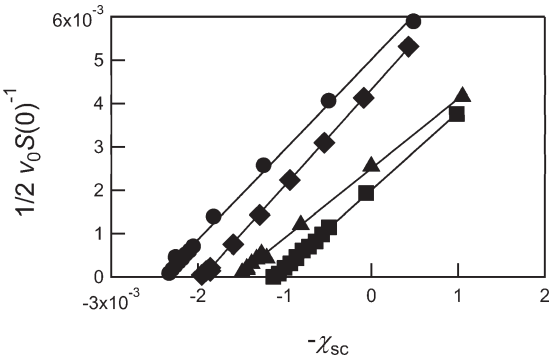

Figure 2. ${}^1/_2 v_0 S(0)^{-1}$ versus $-\chi_{sc}$ for the blend in each series that was prepared at the predicted critical composition: S[0.92] $\phi_{1,crit,pred} = 0.34$ (◆), S[0.72] $\phi_{1,crit,pred} = 0.37$ (●), S[0.29] $\phi_{1,crit,pred} = 0.44$ (■), and S[0.23] $\phi_{1,crit,pred} = 0.47$ (▲). Solid lines are linear fits to the data.

Table 4. Linear Fitting Parameters for the Plots of ${}^1/_2 v_0 S(0)^{-1}$ against $-\chi_{sc}$ Shown in Figure 2[a]

series	S[0.92]	S[0.72]	S[0.29]	S[0.23]
$\phi_{1,crit,pred}$	0.34	0.37	0.44	0.47
intercept	0.00209	0.00266	0.00098	0.00124
slope	1.07	1.10	0.88	0.80

[a] Only the predicted critical blend for each series is shown.

Susceptibility versus $1/T$ plots are shown in Figure 3 for the most and least symmetric series, where symmetry is defined by $N_1/N_2 = 1$. Figure 3a shows plots for the series S[0.92] at the predicted critical composition and at an extremely off-critical composition ($\phi_{1,crit,pred} = 0.34$ and $\phi_1 = 0.77$, respectively). Figure 3b shows the series S[0.23] at $\phi_{1,crit,pred} = 0.47$ and $\phi_1 = 0.73$. For all blends studied, 2 or 3 K temperature steps were used near the phase transition to capture the behavior immediately preceding macrophase separation. As expected, both series show a continuous decrease to zero in the susceptibility at the predicted critical composition. The off-critical blends in Figure 3a,b were prepared at similar compositions for both series; however, they exhibit different behaviors. The susceptibility of S[0.92] with $\phi_1 = 0.77$ decreases discontinuously at $1/T = 0.002\,34\ K^{-1}$. In contrast, the susceptibility of S[0.23] with $\phi_1 = 0.73$ decreases continuously to zero. The latter observation is surprising because we expect a discontinuous jump in the susceptibility when off-critical blends cross the binodal and phase separation is seen after nucleation barriers are crossed. Our observation of S[0.23] with $\phi_1 = 0.73$ indicates that the blend can be superheated all the way to the spinodal.

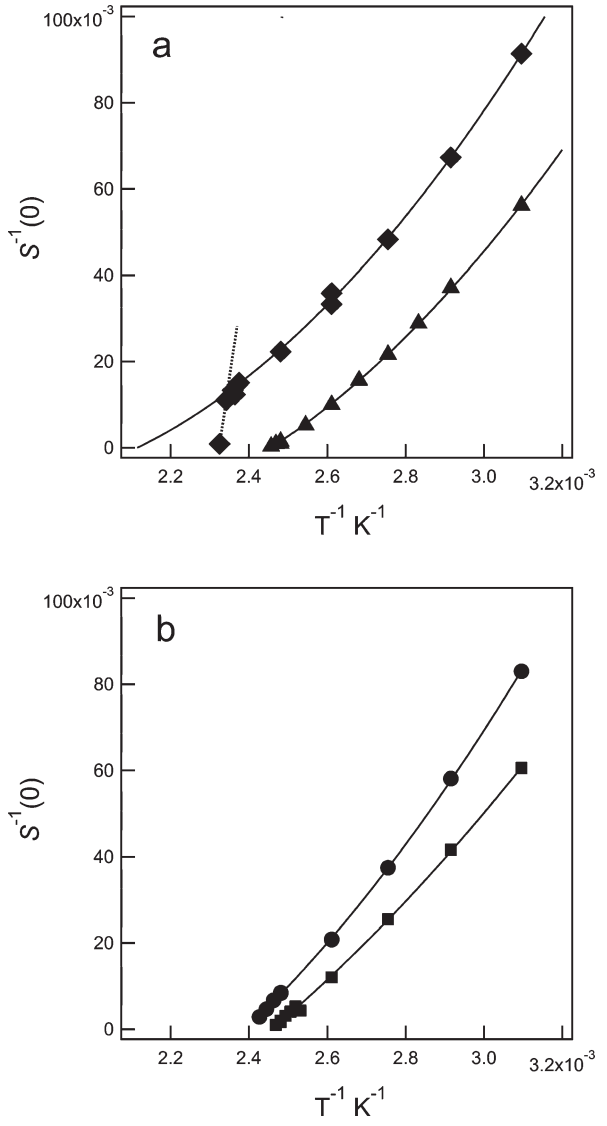

Figure 3. Susceptibility versus inverse temperature for selected blends: (a) S[0.92] series: ϕ_1 = 0.77 (◆) and $\phi_{1,crit,pred}$ = 0.34 (▲) and (b) S[0.23] series with ϕ_1 = 0.73 (●) and $\phi_{1,crit,pred}$ = 0.47 (■). Solid lines are parabolic fits to the data used to obtain T_s, and the dashed line is a linear fit used to obtain T_b.

The binodal temperature is determined from either of two methods using the Ornstein−Zernike fitting parameters. The first method is illustrated in Figure 3a wherein the dotted line represents a linear fit to the susceptibilities measured in the regime where deviations from the quadratic fit are observed. The intersection of this line with the x-axis is taken to be T_b. However, for many off-critical blends studied, the susceptibility does not exhibit any deviation from the quadratic fit, as illustrated in Figure 3b. In this case, T_b was determined as the temperature halfway between the highest temperature that yielded a homogeneous blend and the lowest temperature that yielded a macrophase separated blend. Both methods of measuring T_b were applied to blends with a sharp drop in the susceptibility and yielded the same results (within 2 K).

The main purpose of this paper is to describe the effect of the composition and chain length dependence of χ on phase behavior. Before discussing the phase behavior, it is instructive to gauge the magnitude of departures from the standard Flory−Huggins χ in our system. It is convenient to separate the composition-independent and composition-dependent contributions to the measured χ in eq 18 as follows:

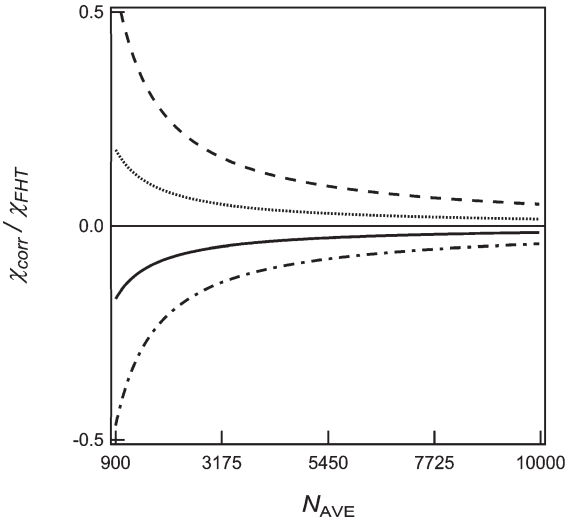

Figure 4. χ_{corr}/χ_{FHT} vs N_{AVE} for ϕ_1 = 0.2 at selected temperatures: 303 K (line), 343 K (dot-dash), 383 K (dash), and 423 K (dots).

$$\chi = \chi_{FHT}(T) + \chi_{corr}(T, \phi_1, N_{AVE}) \qquad (20)$$

χ_{FHT} could be considered as the standard Flory−Huggins parameter that is independent of ϕ_1 and N_i, while χ_{corr} could be considered as a correction to the standard FHT that accounts for the ϕ_1 and N_{AVE} dependence of the overall χ parameter. The polymer blend system studied here exhibits a lower critical solution temperature (LCST); i.e., χ_{FHT} is negative at low temperatures, and it increases with increasing temperature, turning positive at a temperature in the vicinity of 370 K. In contrast, χ_{corr} is positive for $\phi_1 < 0.5$ and negative for $\phi_1 > 0.5$. In Figure 4, we plot χ_{corr}/χ_{FHT} versus N_{AVE} at selected temperatures for a fixed ϕ_1 = 0.2. (Qualitatively similar plots are obtained at other values of ϕ_1.) At temperatures for which χ_{FHT} is negative, χ_{corr}/χ_{FHT} is also negative and changes sign when χ_{FHT} becomes positive. It is evident that behavior consistent with standard Flory−Huggins theory, wherein the magnitude of χ_{corr}/χ_{FHT} is significantly less than unity over the temperature range of interest, is only obtained at N_{AVE} values as large as 10 000. This is well outside the current experimental range of N_{AVE}.

Figure 5 shows the predicted and experimental phase diagrams for each of the blend series. The measured values of T_s and T_b are the data points in Figure 5, and the curves are predictions based on the χ from eq 18. There is an uncertainty associated with the predicted curves due to the uncertainty in χ (eq 18). The error bar on each plot indicates the typical magnitude of this uncertainty. (The error bar corresponds to the estimated error at that point, and the estimated error is a weak function of composition due to the proximity of the binodal and spinodal points in most blends.)

Figure 5a shows the phase behavior of the nearly symmetric S[0.92] series. The measured spinodal and binodal temperatures are coincident in the vicinity of the predicted critical point. The measured values of T_b at the binodal are surprisingly insensitive to changes in ϕ_1. This insensitivity is captured accurately by the predicted binodal curve. There are, however, noteworthy

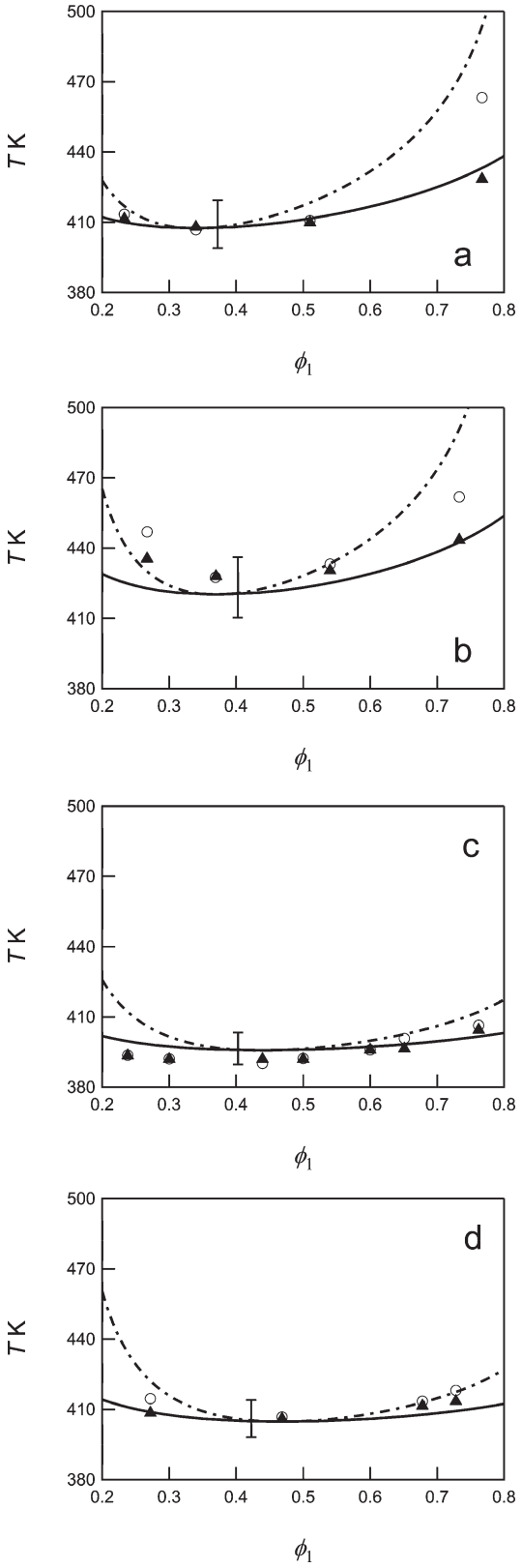

Figure 5. Phase diagrams showing the measured values of T_s (○) and T_b (▲) and the calculated binodal (solid line) and spinodal (dotted line) for (a) S[0.92], (b) S[0.72], (c) S[0.29], and (d) S[0.23]. The error bars in the vicinity of the critical point represent uncertainty in the calculated predicted spinodal and binodal curves due to the uncertainty in χ. The uncertainty in the experimentally determined binodal temperatures is typically less than 2 K and thus comparable to the size of the data points.

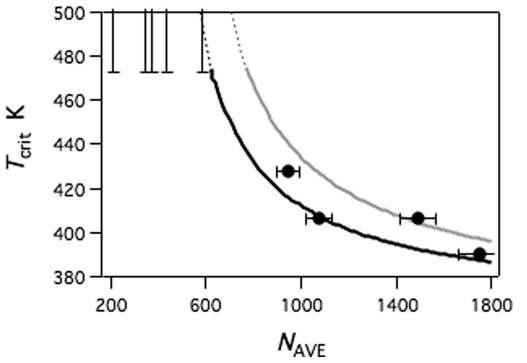

Figure 6. T_{crit} vs N_{AVE} for the four polymer series with $N_{AVE} \geq 950$ (●). The uncertainty in T_{crit} is smaller than the size of the symbols. The lower limit of the error bars for polymer series with $N_{AVE} \leq 580$ is 473 K, the highest temperature probed as these blends did not phase separate in the temperature window 303−473 K. The solid lines are predictions for $N_1/N_2 = 0.92$ (black line) and $N_1/N_2 = 0.23$ (gray line).

departures between the measured and predicted spinodal, particularly at $\phi_1 = 0.77$. The predicted phase diagram in Figure 5a has a shallow minimum at $\phi_1 = 0.34$, which differs from the value of 0.51 that is the critical composition predicted by the standard Flory−Huggins theory. Similar departures from the standard Flory−Huggins theory are seen in the S[0.72] and S[0.23] series, shown in Figure 5b,d. In the case of the S[0.29] series, shown in Figure 5c, the measured values of T_b and T_s are identical over the entire composition window. While the predicted binodal curve is in agreement with the experimental data, the predicted spinodal curve is not.

The predicted critical temperature (T_{crit}) for each PIB/dPBD series, studied here using Flory−Huggins theory, occurs at a temperature in reasonable agreement with the experimental data (Figure 5). While we have focused on blends with $N_{AVE} \geq 950$, we have determined that blends with $N_{AVE} \leq 580$ do not exhibit phase separation over the experimental window 303−473 K. The lower bound for the T_{crit} for blends with $N_{AVE} \leq 580$ is thus 473 K. This information is depicted on a T_{crit} versus N_{AVE} plot shown in Figure 6, where the circles represent data obtained from systems with $N_{AVE} \geq 950$ and the error bars represent the lower bound for the T_{crit} for blends with $N_{AVE} \leq 580$. It is clear that there is a qualitative difference in the phase behavior of blends above and below a certain value of N_{AVE}. T_{crit} increases slowly from 400 to 420 K when N_{AVE} is decreased from 1750 to 950 but then increases rapidly when N_{AVE} is decreased from 950 to 580. This behavior is qualitatively different from predictions based on the standard Flory−Huggins theory but is entirely consistent with the simple expression for χ given in eq 18. The solid lines in Figure 6 represent predictions made for $N_1/N_2 = 0.92$ and 0.23, spanning the experimental range of molecular weight asymmetries presented in this paper. Note that our ability to predict phase behavior at temperatures between 400 and 473 K is entirely due to measurements of the χ parameter from homogeneous blends with $N_{AVE} \leq 580$. The dotted portion of each line extrapolates T_{crit} versus N_{AVE} calculations, assuming that the temperature dependence of χ that we have obtained (eq 18) is applicable at temperatures above 473 K. The kind of qualitative dependence of the phase behavior of polymer blends upon the value of N_{AVE} was anticipated in ref 37 for systems with a χ parameter that exhibits a nonlinear dependence on $1/T$. To our knowledge there are no reports of this in prior literature. It is also

important to contrast the behavior shown in Figure 6 with that for the simple case where $\chi = B/T$ (independent of chain length and composition) wherein the critical temperature is directly proportional to N_{AVE} (ignoring small changes in N_i due to thermal expansion). It should be evident that the nonlinear dependence of χ on $1/T$ and the dependence of χ on ϕ_1 and N_{AVE} are responsible for the trends seen in Figure 6.

Thus far, we have made no attempt to rationalize our experimental observations on the basis of a microscopic picture. Our main new result is that the leading order correction to the standard Flory−Huggins theory decreases relatively slowly with increasing N_{AVE}. There is a large body of theoretical literature wherein microscopic models are used to improve upon the standard Flory−Huggins theory.[27−31] Considerable effort has been focused on the effect of pressure−volume−temperature (PVT) relationships of the pure component and mixtures, local packing in the pure components and mixtures, etc. In fact, the work of Luettmer-Strathmann and Lipson specifically addresses LCST mixtures with PIB as one of the components.[31] It would be interesting to see if predictions of these approaches are consistent with the experimental data presented here. It is well-known, however, that the thermodynamic properties of pure polymers approach their high molecular weight limit when N is of order 10−100 (molecular weights in the range 1−10 kg/mol). It is thus unlikely that these approaches would lead to expressions for the measured χ parameter wherein significant deviations from the standard Flory−Huggins theory are obtained when N is of order 10^4. There is, however, an emerging class of theories pioneered by Wang that suggest that the spectrum of concentration fluctuations in polymer blends is fundamentally different from the predictions of the random phase approximation (RPA), regardless of the local structure of the monomers.[32−36] There is thus a difference between the true χ parameter that must be used in the free energy expression and that inferred by SANS. The phase behavior calculated using the SANS-determined χ is thus predicted to be erroneous. We have found significant deviations between the experimental and predicted spinodals in all of our blends, while there is general agreement between the experimental and predicted binodals. This suggests that the free energy expression used in this work is valid in the stable region where $[\partial^2\Delta G/\partial{\phi_1}^2]_T > 0$ but not in the region where $[\partial^2\Delta G/\partial{\phi_1}^2]_T$ approaches zero. Another interesting conclusion of Wang's predictions is that RPA-like behavior is only recovered when N_i is of order 10^4. While our experiments do not cover this range of N_i values, they do provide indirect support for this prediction (Figure 4).

CONCLUSION

SANS was used to determine the phase behavior of four series of binary PIB/dPBD blends with N_1/N_2 ranging from 0.23 to 0.92 and N_{AVE} ranging from 950 to 1750. To our knowledge, none of the previous studies on polymer blend thermodynamics have covered such a wide range of experimental parameters. The general shapes of the experimentally determined binodal curves were in good agreement with the predictions based on a composition- and chain length-dependent χ parameter presented in ref 17 and given in eq 18. The experimentally determined spinodal curves, which were surprisingly close to the experimental binodal curves, deviated significantly from predictions based on eq 18.

The analysis presented in this paper is based entirely on the Flory−Huggins expression for the free energy of mixing, which is a one-parameter model. It is possible that predictions based on other functional forms for the free energy of mixing (e.g., expressions motivated by the two-parameter models routinely used to describe the thermodynamic properties of small molecule mixtures) will be in better agreement with the experimental data presented here.

ASSOCIATED CONTENT

Supporting Information. Section 1 contains a complete listing of susceptibility and correlation length values, $S(0)$ and ξ, for each blend at each temperature studied; section 2 contrasts the use of mean-field theory with critical scaling law fits in order to determine the spinodal temperature, T_s, from the susceptibility, $S(0)$. This material is available free of charge via the Internet at http://pubs.acs.org.

AUTHOR INFORMATION

Corresponding Author

*E-mail: nbalsara@berkeley.edu; Ph 510 642-8937; Fax 510 642-4778.

ACKNOWLEDGMENT

We acknowledge The Dow Chemical Company for providing the primary support for this work and Dr. T. H. Kalantar for guidance and helpful discussions. A.J.N. was also supported by the Tyco Fellowship. We acknowledge the support of the National Institute of Standards and Technology, U.S. Department of Commerce, in providing the neutron research facilities used in this work. This work utilized facilities supported in part by the National Science Foundation under Agreement No. DMR-0454672.

REFERENCES

(1) Flory, P. J. *J. Chem. Phys.* **1942**, *10*, 51–61.
(2) Huggins, M. L. *J. Phys. Chem.* **1942**, *46*, 151–158.
(3) Crist, B. *J. Polym. Sci., Part B: Polym. Phys.* **1997**, *35*, 2889–2899.
(4) Bates, F. S.; Fetters, L. J.; Wignall, G. D. *Macromolecules* **1988**, *21*, 1086–1094.
(5) Londono, J. D.; Narten, A. H.; Wignall, G. D.; Honnell, K. G.; Hsieh, E. T.; Johnson, T. W.; Bates, F. S. *Macromolecules* **1994**, *27*, 2864–2871.
(6) Schwahn, D.; Hahn, K.; Streib, J.; Springer, T. *J. Chem. Phys.* **1990**, *93*, 8383–8391.
(7) Balsara, N. P.; Lohse, D. J.; Graessley, W. W.; Krishnamoorti, R. *J. Chem. Phys.* **1994**, *100*, 3905–3910.
(8) Reichart, G. C.; Register, R. A.; Graessley, W. W.; Krishnamoorti, R.; Lohse, D. J. *Macromolecules* **1995**, *28*, 8862–8864.
(9) Krishnamoorti, R.; Graessley, W. W.; Balsara, N. P.; Lohse, D. J. *J. Chem. Phys.* **1994**, *100*, 3894–3904.
(10) Balsara, N. P.; Fetters, L. J.; Hadjichristidis, N.; Lohse, D. J.; Han, C. C.; Graessley, W. W.; Krishnamoorti, R. *Macromolecules* **1992**, *25*, 6137–6147.
(11) Han, C. C.; Bauer, B. J.; Clark, J. C.; Muroga, Y.; Matsushita, Y.; Okada, M.; Qui, T. C.; Chang, T. H.; Sanchez, I. C. *Polymer* **1988**, *29*, 2002–2014.
(12) Cabral, J. T.; Higgins, J. S. *Macromolecules* **2009**, *42*, 9528–9536.
(13) Schwahn, D.; Mortensen, K.; Springer, T.; Yeemadeira, H.; Thomas, R. *J. Chem. Phys.* **1987**, *87*, 6078–6087.
(14) deGennes, P. G. In *Scaling Concepts in Polymer Physics*; Cornell University Press: Ithaca, NY, 1979; p 109.

(15) Thudium, R. N.; Han, C. C. *Macromolecules* **1996**, *29*, 2143–2149.
(16) Beaucage, G.; Sukumaran, S.; Clarson, S. J.; Kent, M. S.; Schaefer, D. W. *Macromolecules* **1996**, *29*, 8349–8356.
(17) Nedoma, A. J.; Robertson, M. L.; Wanakule, N. S.; Balsara, N. P. *Macromolecules* **2008**, *41*, 5773–5779.
(18) Sanchez, I. C. *Polymer* **1989**, *30*, 471–475.
(19) Nedoma, A. J.; Robertson, M. L.; Wanakule, N. S.; Balsara, N. P. *Ind. Eng. Chem. Res.* **2008**, *47*, 3551–3553.
(20) Reynolds, B. J.; Ruegg, M. L.; Balsara, N. P.; Radke, C. J.; Shaffer, T. D.; Lin, M. Y.; Shull, K. R.; Lohse, D. J. *Macromolecules* **2004**, *37*, 7401–7417.
(21) Ruegg, M. L.; Reynolds, B. J.; Lin, M. Y.; Lohse, D. J.; Balsara, N. P. *Macromolecules* **2006**, *39*, 1125–1134.
(22) Bates, F. S.; Wignall, G. D.; Koehler, W. C. *Phys. Rev. Lett.* **1985**, *55*, 2425–2428.
(23) Graessley, W. W.; Krishnamoorti, R.; Balsara, N. P.; Fetters, L. J.; Lohse, D. J.; Schulz, D. N.; Sissano, J. A. *Macromolecules* **1993**, *26*, 1137–1143.
(24) Certain commercial equipment, instruments, materials, and suppliers are identified in this paper to foster understanding. Such identification does not imply recommendation or endorsement by the National Institute of Standards and Technology, nor does it imply that the materials or equipment identified are necessarily the best available for the purpose.
(25) Kline, S. R. *J. Appl. Crystallogr.* **2006**, *39*, 895.
(26) Robertson, M. L. Ph.D. Dissertation, University of California, Berkeley, 2006; p 333.
(27) Dudowicz, J.; Freed, M. S.; Freed, K. F. *Macromolecules* **1991**, *24*, 5096–5111.
(28) Schweizer, K. S. *Macromolecules* **1993**, *26*, 6033–6049.
(29) Maranas, J. K.; Mondello, M.; Grest, G. S.; Kumar, S. K.; Debenedetti, P. G.; Graessley, W. W. *Macromolecules* **1998**, *31*, 6991–6997.
(30) Maranas, J. K.; Kumar, S. K.; Debenedetti, P. G.; Graessley, W. W.; Mondello, M.; Grest, G. S. *Macromolecules* **1998**, *31*, 6998–7002.
(31) Luettmer-Strathmann, J.; Lipson, J. E. G. *Macromolecules* **1999**, *32*, 1093–1102.
(32) Muller, M.; Binder, K. *Macromolecules* **1995**, *28*, 1825–1834.
(33) Wang, Z. G. *J. Chem. Phys.* **2002**, *117*, 481–500.
(34) Wittmer, J. P.; Beckrich, P.; Meyer, H.; Cavallo, A.; Johner, A.; Baschnagel, J. *Phys. Rev. E: Stat., Nonlinear, Soft Matter Phys.* **2007**, 11801–11818.
(35) Morse, D. C.; Chung, J. K. *J. Chem. Phys.* **2009**, *130*, 224901.
(36) Jian, Q.; Morse, D. C. *J. Chem. Phys.* **2009**, 224902–224915.
(37) Balsara, N. P.; Eitouni, H. B. In *Physical Properties of Polymer Handbook*, 2nd ed.; Mark, J. E., Ed.; Springer: New York, 2007; pp 339−358.